Available online at www.sciencedirect.com
ScienceDirect
Journal of Organometallic Chemistry 691 (2006) 5505–5512
Journal of Organometallic Chemistry
www.elsevier.com/locate/jorganchem

What difference one double bond makes: Electronic structure of saturated and unsaturated *n*-heterocyclic carbene ligands in Grubbs 2nd generation-type catalysts

Richard L. Lord, Huijun Wang, Mario Vieweger, Mu-Hyun Baik *

Department of Chemistry and School of Informatics, Indiana University, Bloomington, Indiana, USA

Received 11 August 2006; received in revised form 7 September 2006; accepted 7 September 2006
Available online 26 September 2006

Abstract

N-heterocyclic carbene (NHC) ligands are a versatile and useful class of ligands that have enjoyed much success over the past few decades in organometallic chemistry. This fact is exemplified most convincingly in Grubbs 2nd generation olefin metathesis catalysts. We explore the electronic impact of the NHC-ligand by decoupling electronic and steric effects through simplified model N-heterocyclic carbenes. Saturated and unsaturated N-heterocyclic carbene ligands give rise to fundamentally different frontier orbitals in these catalysts, suggesting a need to classify them as two electronically distinct ligand classes.

Keywords: N-heterocyclic carbene ligand; Ruthenium; Grubbs catalyst; Olefin metathesis

1. Introduction

The remarkable olefin metathesis catalysts developed by Grubbs [1] are an inspiration for many in the field of catalyst design. Whereas understanding the catalytic mechanism with the goal of further optimizing the catalyst and expanding the scope of its activity is a formidable goal, the underlying electronic structure of the catalyst is also broadly interesting from more fundamental perspectives. For example, in the widely accepted Chauvin mechanism [2] (Eq. (1)) the olefin-adduct, formally a 16-electron species,

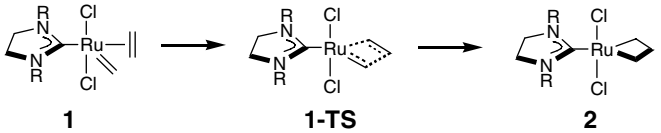

(1)

undergoes a [2+2] cycloaddition to yield a metallacyclobutane intermediate, formally a 14-electron species. Classical organometallic logic predicts the 14-electron intermediate to be higher in energy than the 16-electron analogue. Computational [3–6] and experimental [7] studies suggest, however, that the 14-electron intermediate is lower in energy than the 16-electron reactant complex. We proposed recently that one of the factors contributing to the thermodynamic stability of the metallacyclobutane is a thus far not recognized agostic interaction that we termed α,β-(C–C–C)-agostic to denote the fact that the two C–C σ-bonds are donating electron density to the metal center [8].

The remarkable increase of both activity and versatility of the catalyst [9–11] when one of the phosphine ligands [12] is replaced with an N-heterocyclic carbene (NHC) ligand illustrates the importance of ligand variation in catalyst tuning. NHC-ligands [13–15] are interesting for many reasons, one of the most important being that they provide substantially more opportunities for ligand functionalization than the phosphine ligands with distinctively different functionalization sites on the five-membered ring, which in turn enables more flexible rational design, in principle. The reason that the Grubbs second generation catalysts outperform their predecessors is generally believed to be due to a lower [2 + 2] cyclization barrier compared to the first

* Corresponding author.
E-mail address: mbaik@indiana.edu (M.-H. Baik).

0022-328X/$ - see front matter © 2006 Elsevier B.V. All rights reserved.
doi:10.1016/j.jorganchem.2006.09.036

generation catalysts leading to more rapid and cleaner completion of the metathesis reaction [16,17]. Many aspects of the olefin metathesis reaction have been examined utilizing computational methods in the past and a number of electronic structure studies appeared in the literature discussing the nature of the NHC-ligand [18–25]. In this work, we make use of high-level density functional theory to examine the molecular orbital diagram of the 2nd generation Grubbs catalyst and highlight the structure–reactivity relationship by using simplified models of the NHC-ligands, where both the saturated and unsaturated NHC-ligands are taken into account [26]. We examine how functionalizing the NHC-ligand at the N-positions with electron-donating and electron-withdrawing groups, represented by CH_3 and F ligands, respectively, influences the [2 + 2] cyclization reaction.

2. Computational details

All calculations were carried out using Density Functional Theory as implemented in the Jaguar 6.0 suite of *ab initio* quantum chemistry programs [27]. Geometry optimizations were performed at the B3LYP/6-31G** level of theory [28–31], with transition metals represented using the Los Alamos LACVP basis that includes relativistic effective core potentials [32–34]. Whereas this level of theory has been shown to generate reasonable structures, we found in previous studies that the energies cannot be trusted [8,35,36]. Thus, the energies were reevaluated using Dunning's correlation-consistent triple-ζ basis set cc-pVTZ(-f) [37] at the previous geometry. For all transition metals, we use a modified version of LACVP, designated as LACV3P, where the exponents were decontracted to match the effective core potential with a triple-ζ quality basis. This protocol represents a reasonable compromise between numerical accuracy and computational cost. Solvation energies for molecules were computed using a continuum solvation model [38,39], with a dielectric constant of 9.08 simulating dichloromethane. Solvation energies and vibrational calculations were computed at the B3LYP/LACVP** level of theory. All stationary points were confirmed to be minima by checking the harmonic frequencies. Thermodynamic properties were calculated as summarized below, where we assume standard approximations for deriving the entropy corrections in gas phase. Note that the solution phase free energy is obtained by simply adding the free energy of solvation obtained by the continuum model to the gas phase free energy.

$$\Delta H(\text{gas}) = \Delta E(\text{SCF}) + \Delta\text{ZPE} \quad (2)$$

$$\Delta G(\text{gas}) = \Delta H(\text{gas}) - (298.15K)\Delta S(\text{gas}) \quad (3)$$

$$\Delta G(\text{sol}) = \Delta G(\text{gas}) + \Delta G_{\text{solv}} \quad (4)$$

$\Delta H(\text{gas})$ = gas phase enthalpy; $\Delta E(\text{SCF})$ = electronic energy computed in the self-consistent-field calculation; ΔZPE = Zero-Point-Energy correction; $\Delta G(\text{gas})$ = gas phase free energy; $\Delta S(\text{gas})$ = gas phase entropy; $\Delta G(\text{sol})$ = solution phase free energy; ΔG_{Solv} = free energy of solvation.

Transition states were located on the potential energy surface by first obtaining an approximate structure using the linear synchronous transit method (LST) [40], followed by a quadratic synchronous transit (QST) [41] search using the LST transition state as an initial guess structure. In QST, the initial part of the transition state search is restricted to a circular curve connecting the reactant, initial transition state guess and the product, followed by a search along the Hessian eigenvector that is most similar to the tangent of this curve. Vibrational calculations on the resulting transition state structures, utilizing analytical second derivatives at the B3LYP/LACVP** level, confirmed each transition state to be a first-order saddle point with one imaginary frequency. Zero-point-energy (ZPE) and entropy corrections were derived using the unscaled frequencies from these calculations.

3. Results and discussion

3.1. Structure and bonding of NHC–Ru complexes

One of the notable structural characteristics of the Grubbs catalyst is the sterically demanding 1,3,5-trimethylphenyl group at the N-positions of the NHC-ligand. Whereas sterically shielding the reactive metal site is plausible for enhancing the reactivity, it is not clear whether or not there is also an electronic component in how these functional groups influence the reactivity. Secondly, a common structural variation of the NHC-ring is to introduce one additional C–C double bond to afford the unsaturated analogue. Previous work [26] established that the saturated NHC-ligands are better donor ligands than their unsaturated analogues, but it is thus far not clear how the π-resonance impacts the metal–ligand interaction pattern and how that difference changes the [2 + 2] cycloaddition profile.

Fig. 1 illustrates the optimized structures of the six models and the key structural parameters are given in Table 1. The Ru-carbene bond lengths indicate that the saturated heterocycle with an electron withdrawing group, **2a**, is the most tightly binding ligand, which may be attributed to a stronger π-interaction (*vide infra*). Interestingly, the simplest NHC-ligands **2b′** and **4b′** prefer to adopt fairly coplanar geometries relative to the Cl–Ru–Cl axis with dihedral angles of 26.6° and 0.9°, respectively. To generate a consistent set of models that will allow for a direct and fair comparison, we generated hypothetical structures where we rotated the NHC-ligand by 90°. These pseudo-catalysts are labeled as **2b** and **4b**, respectively, throughout the study (Scheme 1).

The fluorinated NHC-systems **2a** and **4a** show an orthogonal arrangement with dihedral angles of 95.3° and 88.4°, respectively. The methyl-substituted models **2c** and **4c** display intermediate dihedral angles of 80.9° and 64.1°,

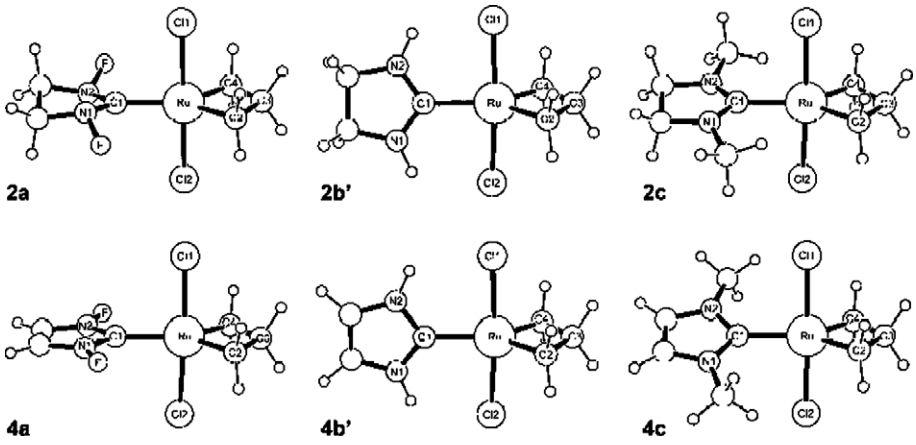

Fig. 1. Optimized structures of the metallacyclobutane models.

Table 1
Key bond lengths listed in Å for the fully relaxed metallacyclobutane models

Bond/Å	2a	2b′	2c	4a	4b′	4c
Ru–C1	1.991	2.061	2.025	2.038	2.048	2.047
C1–N1	1.350	1.333	1.341	1.344	1.350	1.355
C1–N2	1.351	1.333	1.340	1.344	1.350	1.355
Ru–C2	1.974	1.974	1.977	1.969	1.972	1.975
Ru–C3	2.268	2.270	2.283	2.254	2.262	2.272
Ru–C4	1.973	1.974	1.977	1.969	1.972	1.972
C2–C3	1.586	1.587	1.584	1.587	1.590	1.584
C4–C3	1.588	1.587	1.584	1.587	1.588	1.586
NHC-dih. angle[a]	95.3	26.6	80.9	88.4	0.9	64.1

[a] The NHC-angle denotes the dihedral angle defined by the atoms Cl1–Ru–C1–N1.

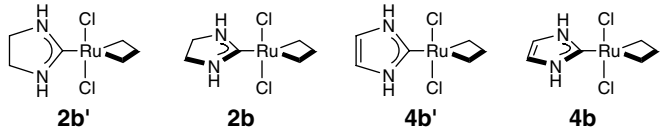

Scheme 1.

respectively. The markedly different dihedral angles of the sterically comparable demanding fluorine and methyl groups, particularly when the NHC-ligand is unsaturated (**4a** and **4c**), suggest that significant electronic effects that are dependent on the N-functionalization are present. Clearly the much greater steric demands of the 1,3,5-trimethylphenyl group in the Grubbs catalyst will enforce the orthogonal NHC-arrangement and overwrite any electronic effects that may exist. Examining the hypothetical small model complexes that we discuss herein more clearly distinguishes the electronic effects that govern the reactivity.

Fig. 2 shows a simplified MO-diagram of the four models shown in Scheme 1 (**2b′**, **2b**, **4b′**, **4b)**. Isosurface plots of the key MOs are given in Fig. 3. Whereas the overall electronic structure is of course similar in all four systems, significant differences exist both for the saturated versus unsaturated and the parallel versus orthogonal arrangement of the NHC-ligands. As expected for a Ru(IV)-d^4 system, two metal-dominated frontier orbitals in the metal–ligand non/anti-bonding manifold are occupied, with the HOMO being mostly metal–d_{yz}. The second highest occupied MO is the complementary π-orbital, dominated by d_{xz}. In the case of the saturated NHC-ligands, the most pronounced dependence on the rotational angle of the carbene ligand is observed for the M–L bonding and antibonding MOs with d_{xy} character. MO-42 of **2b′** shows strong coupling to the NHC π-system, with the metal–d_{xy} orbital forming an in-phase combination with the π-orbital of the NHC-fragment. The isosurface plot in Fig. 3 illustrates that this MO is what was previously recognized as the key MO promoting the α,β-(C–C–C) agostic bond [8]. Note that this is not a classical π-backdonation type of interaction, as it is not the π*-orbital of the NHC-ligand that is involved, but rather the π-orbital with one node. Thus, MO-42 contributes to delocalizing the α,β-(C–C–C) agostic bond, which weakens the agostic interaction within the metallacyclobutane fragment as electron density is removed from the metallacycle. This electronic feature may be one of the reasons why steric bulk at the NHC-ligand and the coplanar arrangement of the NHC-ring with the metallacycle is advantageous electronically. Upon rotating the NHC-ligand by 90° to afford **2b**, in which the NHC-ligand is approximately orthogonal to the Cl–Ru–Cl axis, the coupling of Ru–d_{xy} orbital to the NHC-ligand disappears due to symmetry mismatch, as shown in MO-43 of **2b** (bottom right hand entry in Fig. 3). Similar dependence is seen in the antibonding MOs, MO-57 for **2b′** and its corresponding MO-58 for **2b**. It is plausible to expect that the d_{xz}-dominated MOs would interact with the NHC-π orbitals, since their symmetries would allow such interaction. To our surprise, we found that there is practically no communication between the d_{xz} frontier orbitals and the NHC-π

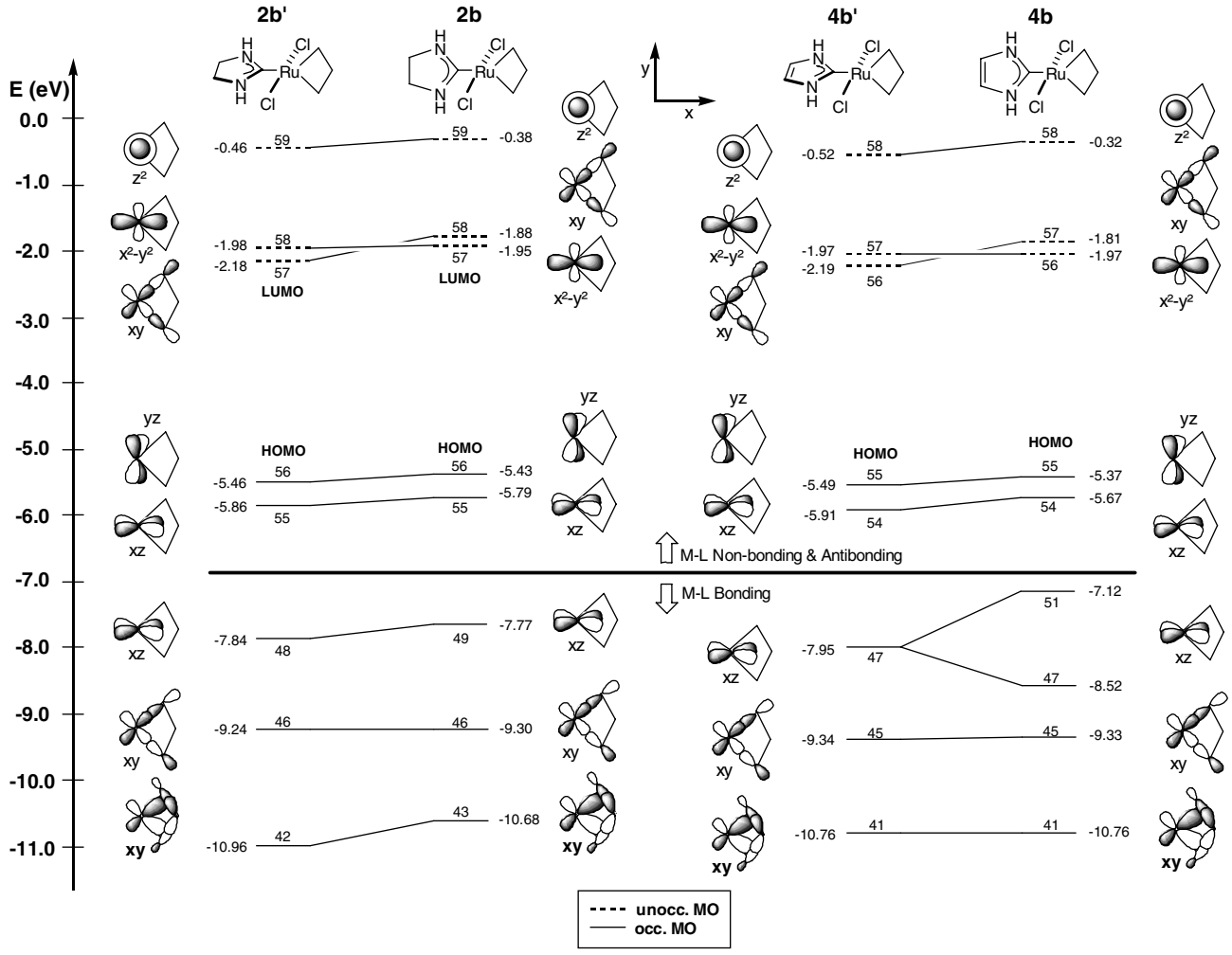

Fig. 2. MO-diagram comparing the most important MOs of **2b′**, **2b**, **4b′** and **4b**.

orbitals. As shown in Fig. 3, NHC-based orbitals do not contribute to MO-48 and MO-55 in **2b′**. Similarly, we found negligible mixing of NHC-based orbitals with the corresponding MOs, MO-49 and MO-55, in **2b**. Overall, the unsaturated NHC-ligand interacts in a similar fashion with the Ru-center, as shown in Fig. 2. However, a markedly different electronic feature arises from the π-resonance, which enhances the ability of the NHC-ligand to interact with the metal-center. Upon rotation of the NHC-ligand, MO-47 of **4b′**, the metal–ligand π-bonding with the Cl^- ligands forms the in-phase and out-of-phase combinations with the π-orbitals of the NHC-ligand to afford MO-47 and MO-51 (Fig. 4). As seen for the saturated NHC-ligand, the ligand π-orbitals involved in this interaction are the filled π-orbitals. The complete lack of rotational dependence of the α,β-(C–C–C) agostic bonding orbital, MO-41 (Fig. 2) in **4b′**/**4b**, is surprising. This naturally led to the question: Why is the α,β-(C–C–C) agostic bond only affected by the rotation of the NHC when the heterocycle is saturated?

The additional double bond in the NHC-ring gives rise to a resonance stabilized ligand, in which there are three occupied and two unoccupied π-orbitals. In the saturated NHC-ligand, however, there are only two filled and one empty π-orbital. The MO-diagram in Fig. 5 illustrates quantitatively this difference. The HOMO of the unsaturated NHC-ligand at an orbital energy of −6.014 eV has the correct symmetry to interact with the metal center affording MOs 47 and 51 (Fig. 2, right hand side), whereas the HOMO of the saturated NHC-ligand at −6.012 eV has the appropriate energy, but the wrong symmetry to interact. The only other π-orbital at −8.902 eV, which has the correct symmetry, cannot participate in bonding because it is too low in energy. Thus, MO-49 of **2b** (Fig. 2) has no contribution from the NHC-ligand. It is the out-of-phase combination with the additional double-bond that enables this π-interaction by raising the ligand π-orbital energy, as illustrated in Fig. 5. Thus, our calculations indicate that the electronic features in the π-orbital space are substantially different between the saturated and unsat-

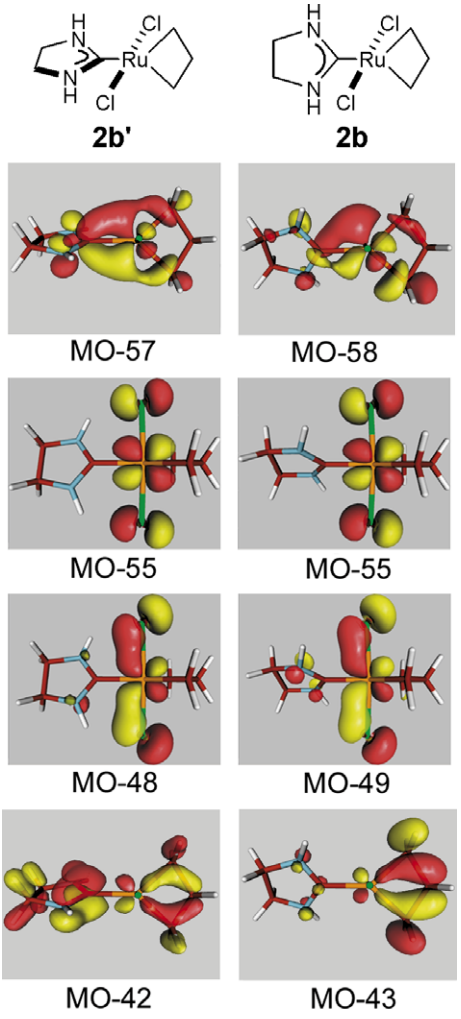

Fig. 3. Isosurface plots of the most important MOs in **2b**′ and **2b** (isodensity = 0.05 a.u.).

urated NHC-ligands, suggesting that the unsaturated NHC-ligands should be considered a different class of ligands. The degree of delocalization of the π-orbital space also suggests that the unsaturated NHC-ligand should allow for greater electronic control by functionalization, in general.

3.2. Reaction profiles for different NHC backbones

To quantify the effect of the different functional groups and the presence of the additional double bond in the NHC-ring on the reactivity of the catalyst, we have computed the key steps of the reaction starting from the olefin adduct. Figs. 6 and 7 show the reaction free energy profiles for the saturated and unsaturated NHC-ligands, respectively. The reaction profiles of **1b** and **1c** are practically identical with an activation free energy of ~3 kcal/mol, which is in good agreement with the previously reported value of ~4.5 kcal/mol for a large model of the 2nd generation Grubbs catalyst [22]. The metallacyclobutane intermediate is found roughly at −4.5 kcal/mol relative to the olefin adduct. Interestingly, the electron-withdrawing fluoro-group lowers the activation barrier significantly by ~2 kcal/mol to give an activation free energy of only 1.05 kcal/mol. The relative energy of the metallacyclobutane intermediate is less sensitive towards functionalization, however. Solvation, modeled in this work using a continuum model with the dielectric constant set to 9.08

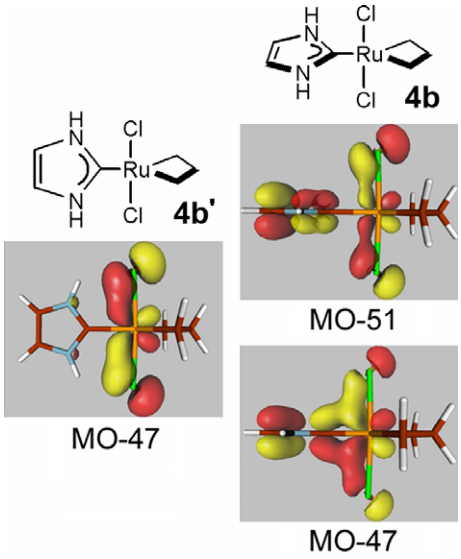

Fig. 4. Isosurface plots of the occupied π-orbitals with significant metal–ligand interaction in **4b**′ and **4b** (isodensity = 0.05 a.u.).

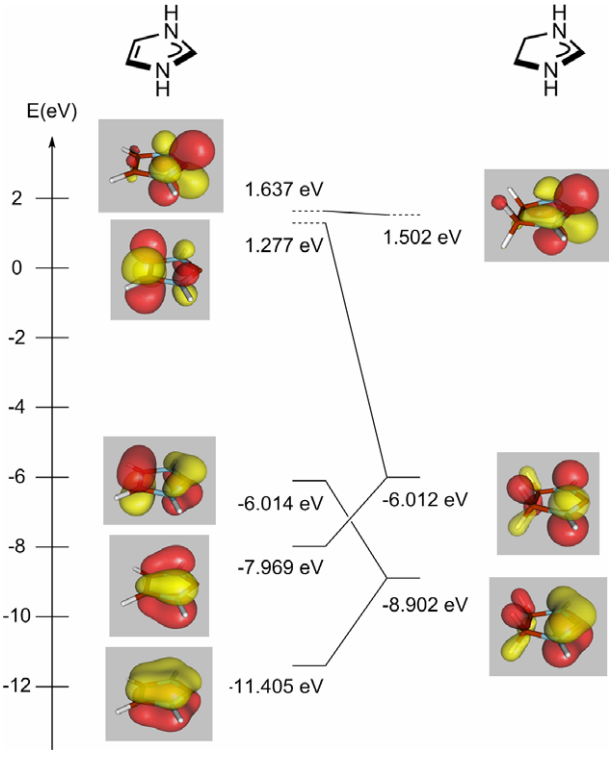

Fig. 5. Isosurface plots of the occupied and unoccupied π-orbitals of the NHC-ligands.

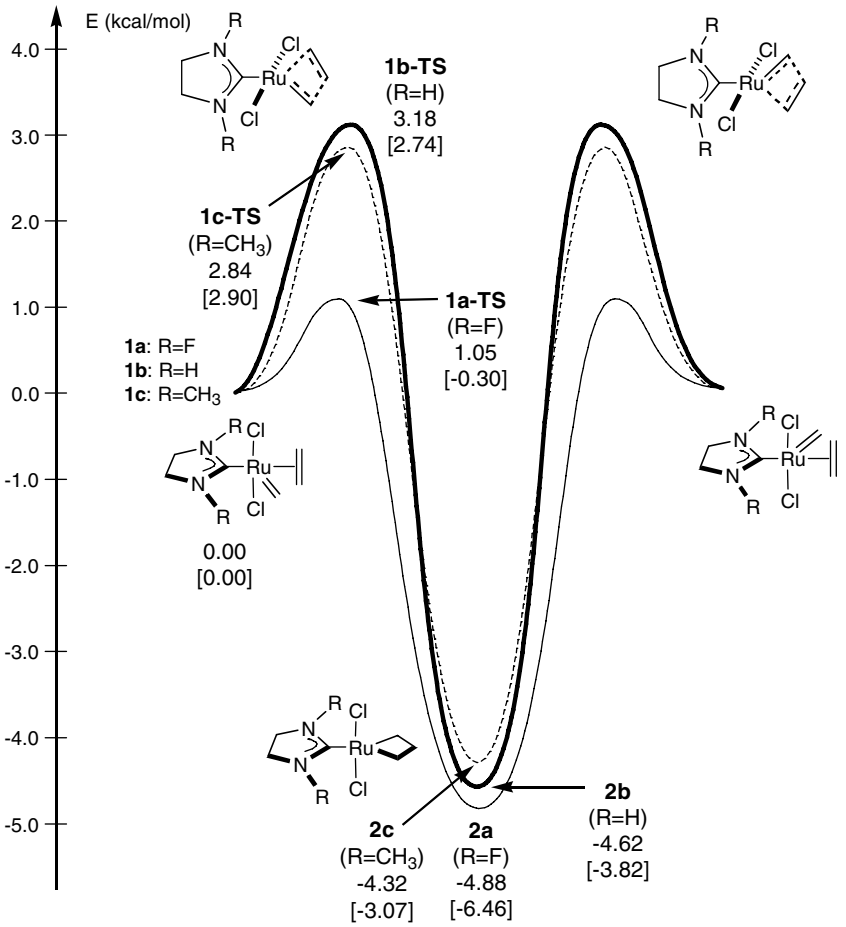

Fig. 6. Computed reaction free energy profile in gas phase using the saturated NHC-ligands. Solution phase numbers are given in square brackets.

(dichloromethane), has only a minor impact on the reaction energy profile, except in the case of the fluoro-analogue, where both the transition and intermediate states are lowered in energy by 1.35 and 1.58 kcal/mol, respectively. As a consequence, the transition state **1a**–**TS** becomes lower in energy than the olefin adduct **1a** in solution phase. Although these absolute energies should not be overinterpreted, these calculations indicate that electron-withdrawing groups at the N-position of the NHC-ligand lower the activation energy of the [2 + 2] reaction significantly without having the same effect on the stability of the metallacycle. For optimizing the performance of the olefin metathesis catalyst it is important to lower the activation barrier without lowering the intermediate energy to the same extent, as the next step in the metathesis reaction requires the metallacycle to reform the olefin adduct.

The reaction energy profiles of the unsaturated NHC-ligands are significantly different from those of the saturated NHC-ligands, as shown in Fig. 7. The reaction energy profiles are much more dependent on the functional groups than seen in the saturated NHC-analogues with relative energies of the metallacycle ranging from 2.6 to −5.2 kcal/mol. The activation free energies are also spread over an energy range of 5 kcal/mol from 2.5 to 7.5 kcal/mol. Unlike in the case of the saturated NHC-ligand, the fluoro-substituent increases the activation barrier and the metallacycle intermediate is higher in energy than the olefin adduct. This dramatic dependence of the reaction energy profiles is of course a direct consequence of the higher degree of electronic communication introduced by the extended π-system. Overall, our calculations suggest that the saturated NHC-ligand system with electron-withdrawing substituents at the N-positions display the most desirable reaction profile pattern, i.e. low lying transition state and relatively high-lying intermediate. Interestingly, the fluoro-substituted, unsaturated NHC-ligand affords a reaction energy profile where the metallacycle is energetically higher than the olefin adduct, giving access to a qualitatively different reaction energy profile. The highest barrier of the metathesis step thus becomes the formation of the metallacycle (**3a** → **3a-TS**), instead of the consumption of the metallacycle (e.g. **4b** → **3b-TS**), as in all other cases.

4. Conclusions

Model systems of Grubbs 2nd generation catalysts have been investigated with high-level density functional theory.

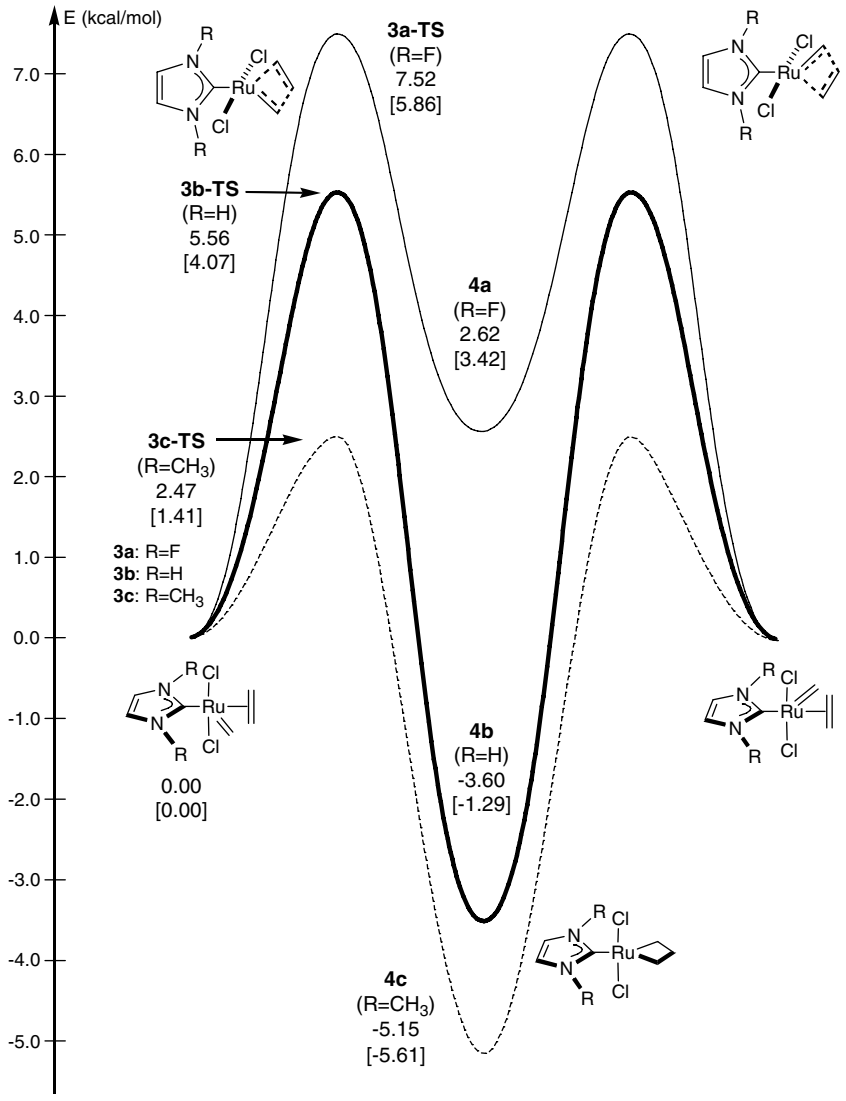

Fig. 7. Computed reaction free energy profile in gas phase using the unsaturated NHC-ligands. Solution phase numbers are given in square brackets.

Rotational preference of the NHC in the experimental system, which is forced to be perpendicular due to the bulky mesityl substituents at the N-positions of the NHC-ring, is proposed not only to be advantageous due to shielding of the reactive metal site, but to be of fundamental importance to the thermodynamic stability of the metallacyclobutane intermediate and ultimately the overall shape of the reaction energy profiles. Additionally, our investigation of the frontier orbital manifolds of these systems displays clear differences between the 1st and 2nd generation catalysts when compared to our previous work. Ruthenium–metallacyclobutane bonding is weaker in the NHC complexes, displayed by the more positive metal–ligand bonding orbital energies. This observation reflects on the well accepted propensity of N-heterocyclic carbenes to donate more electron density than phosphines, helping to relieve the strain on the electron–poor ruthenium center. This translates into more facile bond breaking and bond forming in the metathesis mediated by the 2nd generation catalysts. Both ligand types investigated here display interesting bonding motifs with the metallacyclobutane fragment, particularly with respect to rotation, with metal–ligand bonding arising from interactions with the π-system instead of the expected π^*-system.

Acknowledgement

We thank the National Institutes of Health (HG-003894), the Research Corporation (Cottrell Scholar Award) and the National Science Foundation (0116050 to Indiana University) for financial support.

Appendix A. Supplementary data

Supplementary data associated with this article can be found, in the online version, at doi:10.1016/j.jorganchem.2006.09.036.

References

[1] R.H. Grubbs, Angew. Chem., Int. Ed. Engl. 45 (2006) 3760–3765.
[2] J.L. Herisson, Y. Chauvin, Makromol. Chem. 141 (1971) 161–176.
[3] C.H. Suresh, N. Koga, Organometallics 23 (2004) 76–80.
[4] S.E. Vyboishchikov, M. Buhl, W. Thiel, Chem. Eur. J. 8 (2002) 3962–3975.
[5] C. Costabile, L. Cavallo, J. Am. Chem. Soc. 126 (2004) 9592–9600.
[6] J.J. Lippstreu, B.F. Straub, J. Am. Chem. Soc. 127 (2005) 7444–7457.
[7] P.E. Romero, W.E. Piers, J. Am. Chem. Soc. 127 (2005) 5032–5033.
[8] C.H. Suresh, M.-H. Baik, Dalton Trans. (2005) 2982–2984.
[9] M. Scholl, S. Ding, C.W. Lee, R.H. Grubbs, Org. Lett. 1 (1999) 953–956.
[10] C.W. Bielawski, R.H. Grubbs, Angew. Chem. Int. Ed. Engl. 39 (2000) 2903–2906.
[11] T.M. Trnka, R.H. Grubbs, Acc. Chem. Res. 34 (2001) 18–29.
[12] E.L. Dias, S.T. Nguyen, R.H. Grubbs, J. Am. Chem. Soc. 119 (1997) 3887–3897.
[13] A.J. Arduengo, Acc. Chem. Res. 32 (1999) 913–921.
[14] A.J. Arduengo, H.V.R. Dias, R.L. Harlow, M. Kline, J. Am. Chem. Soc. 114 (1992) 5530–5534.
[15] A.J. Arduengo, R.L. Harlow, M. Kline, J. Am. Chem. Soc. 113 (1991) 361–363.
[16] M.S. Sanford, J.A. Love, R.H. Grubbs, J. Am. Chem. Soc. 123 (2001) 6543–6554.
[17] M.S. Sanford, M. Ulman, R.H. Grubbs, J. Am. Chem. Soc. 123 (2001) 749–750.
[18] D.A. Dixon, A.J. Arduengo, J. Phys. Chem. 95 (1991) 4180–4182.
[19] D.A. Dixon, A.J. Arduengo, J. Phys. Chem. A 110 (2006) 1968–1974.
[20] R. Dorta, E.D. Stevens, N.M. Scott, C. Costabile, L. Cavallo, C.D. Hoff, S.P. Nolan, J. Am. Chem. Soc. 127 (2005) 2485–2495.
[21] C. Adlhart, P. Chen, Helv. Chim. Acta 86 (2003) 941–949.
[22] C. Adlhart, P. Chen, J. Am. Chem. Soc. 126 (2004) 3496–3510.
[23] A.C. Tsipis, A.G. Orpen, J.N. Harvey, Dalton Trans. (2005) 2849–2858.
[24] G. Occhipinti, H.-R. Bjorsvik, V.R. Jensen, J. Am. Chem. Soc. 128 (2006) 6952–6964.
[25] B.F. Straub, Angew. Chem. Int. Ed. Engl. 44 (2005) 5974–5978.
[26] A.C. Hillier, W.J. Sommer, B.S. Yong, J.L. Petersen, L. Cavallo, S.P. Nolan, Organometallics 22 (2003) 4322–4326.
[27] Jaguar 6.0, Schrödinger, Inc., Portland, Oregon, 2003.
[28] A.D. Becke, Phys. Rev. A 38 (1988) 3098–3100.
[29] A.D. Becke, J. Chem. Phys. 98 (1993) 5648–5652.
[30] C. Lee, W. Yang, R.G. Parr, Phys. Rev. B 37 (1988) 785–789.
[31] S.H. Vosko, L. Wilk, M. Nusair, Can. J. Phys. 58 (1980) 1200–1211.
[32] P.J. Hay, W.R. Wadt, J. Chem. Phys. 82 (1985) 270–283.
[33] W.R. Wadt, P.J. Hay, J. Chem. Phys. 82 (1985) 284–298.
[34] P.J. Hay, W.R. Wadt, J. Chem. Phys. 82 (1985) 299–310.
[35] M.-H. Baik, R.A. Friesner, J. Phys. Chem. A 106 (2002) 7407–7415.
[36] M.H. Baik, E.W. Baum, M.C. Burland, P.A. Evans, J. Am. Chem. Soc. 127 (2005) 1602–1603.
[37] T.H. Dunning Jr., J. Chem. Phys. 90 (1989) 1007–1023.
[38] B. Marten, K. Kim, C. Cortis, R.A. Friesner, R.B. Murphy, M.N. Ringnalda, D. Sitkoff, B. Honig, J. Phys. Chem. 100 (1996) 11775–11788.
[39] D.J. Tannor, B. Marten, R.B. Murphy, R.A. Friesner, D. Sitkoff, A. Nicholls, M.N. Ringnalda, W.A. Goddard III, B. Honig, J. Am. Chem. Soc. 116 (1994) 11875–11882.
[40] T.A. Halgren, W.N. Lipscomb, Chem. Phys. Lett. 49 (1977) 225–232.
[41] C.Y. Peng, H.B. Schlegel, Isr. J. Chem. 33 (1993) 449–454.